semiconductor film.[8] The volume fraction of particles, F, was assessed from[9]

$$\frac{n_s^2 - n_m^2}{n_s^2 + 2n_m^2} = F\left(\frac{n_B^2 - n_m^2}{n_B^2 + 2n_m^2}\right) \quad (2)$$

where n_B and n_m are the refractive indexes of bulk crystalline semiconductors (Table I) and the surrounding medium. It is interesting to note that different particulate semiconductors organize themselves to different packing (see F values in Table I).

The semiconductor particulate films, formed at the mono- and poly[(vinylbenzyl)phosphonate] interfaces, were transferred to solid substrates by horizontal lifting. Well-cleaned quartz (chromic acid and dust-free water), celluloid-coated copper grids, and highly oriented pyrolytic graphite (HOPG, Union Carbide, freshly cleaved) were used for absorption spectrophotometry, transmission microscopy, and scanning tunneling microscopy, respectively.

Optical thicknesses of films on quartz prisms were also determined by reflectivity measurements. The optical thickness of a given particulate film on a glass prism was only 4–6% smaller than that determined on the monolayer surface prior to its transfer.

Absorption spectra of typical CdS and ZnS particulate films are shown in Figure 2. The simultaneous presence of fine structures (maxima and shoulders) and absorption edges situated at relatively long wavelengths is explicable by assuming the presence of a broad distribution of semiconductor particles, ranging from ultrasmall size-quantized[10] to relatively larger ones, in the particulate films. The broad size distribution, already observed in the thinnest film, remained essentially unaltered in the thicker films formed from the same semiconductor. Direct bandgaps, E_g values, were obtained from the intercepts of plots of the data according to eq 3, where σ is the ab-

$$(\sigma h\omega)^2 = h\omega C - E_g C \quad (3)$$

sorption coefficient ($A = \sigma d$ where A is the absorbance and d is the optical thickness of the semiconductor particulate film determined from reflectivity measurements) and $h\omega$ is the photon energy. Typical plots of the left-hand side of the equation against $h\omega$ are also shown in Figure 2. Values of E_g for CdS particulate films of d = 75, 130, 180, and 330 Å were assessed to be 2.59 (478 nm), 2.56 (485 nm), 2.49 (498 nm), and 2.44 eV (507 nm). Similarly, E_g values of ZnS particulate films of d = 110, 180, and 280 Å were calculated to be 3.71 (334 nm), 3.69 (336 nm), and 3.67 eV (338 nm). Values of 2.2 (558 nm) and 3.84 eV (323 nm) were similarly derived for the 270-Å-thick PbS and the 350-Å-thick In_2S_3 particulate films.

Transmission electron microscopy indicated the predominance of 75- and 80-Å-diameter particles of CdS and ZnS (Figure 3). In contrast, PbS appeared to form large cubic microcrystalline structures and the initially formed, very small In_2S_3 particles appeared to aggregate to larger structures (Figure 3).

Thin semiconductor particles, deposited on HOPG, were imaged in air by scanning tunneling microscopy (STM) using an Angstrom Technology (Mesa, AZ) Tak 3.0 instrument operated in the constant-current (1.0 nA) mode. STM images were scanned at five lines per second at ±500 mV tunneling voltage (tip vs substrate) and plotted on a CP 200 U Mitsubishi color video processor. STM images were taken on several separately prepared samples, and for each sample, data were taken at 10 different areas. The observed images showed particles with 20–30-Å widths and heights, which often formed loosely interconnecting structures (Figure 4).

In summary, functionalized monolayers have been shown to provide highly suitable matrices for the preparation of size-quantized particulate semiconductor films that could be transferred to a solid support. The methodology described here will allow the development of unique, nanosized electronic devices whose construction and examination are the subject of our current and intense scrutiny.

Acknowledgment. Support of this research by funds from the Center for Membrane Engineering and Science at Syracuse University is gratefully acknowledged.

(8) Zhao, X. K.; Baral, X.; Fendler, J. H. *J. Phys. Chem.* **1990**, *94*, 2043.

(9) Garnett, M. S. C. *Philos. Trans. R. Soc. London* **1904**, *203*, 385.

(10) Henglein, A. *Top. Curr. Chem.* **1988**, *143*, 113. Brus, L. A. *J. Phys. Chem.* **1986**, *90*, 2555. Andres, R. P.; Averback, R. S.; Brown, W. L.; Brus, L. E.; Goddard, W. A.; Kaldor, A.; Louie, S. G.; Moskovits, M.; Percy, P. S.; Riley, S. J.; Siegel, R. W.; Spaepen, F.; Wang, Y. *J. Mater. Res.* **1989**, *4*, 704.

Chromophore-Functionalized Polymeric Thin-Film Nonlinear Optical Materials. Effects of in Situ Cross-Linking on Second Harmonic Generation Temporal Characteristics

Joonwon Park and Tobin J. Marks*

Department of Chemistry and the Materials Research Center Northwestern University, Evanston, Illinois 60208

Jian Yang and George K. Wong*

Department of Physics and the Materials Research Center Northwestern University, Evanston, Illinois 60208

Received January 12, 1990

By increasing realizable chromophore number densities while impeding structural disorientation processes following electric field poling, chromophore-functionalized glassy polymers[1-3] represent an advance in macromolecular second harmonic generation (SHG) materials.[4] Nevertheless, structural relaxation/physical aging processes,[5,6] which erode poling-induced noncentrosymmetry and hence limit

(1) (a) Ye, C.; Marks, T. J.; Yang, Y.; Wong, G. K. *Macromolecules* **1987**, *20*, 2322–2324. (b) Ye, C.; Minami, N.; Marks, T. J.; Yang, J.; Wong, G. K. *Macromolecules* **1988**, *21*, 2901–2904. (c) Ye, C.; Minami, N.; Marks, T. J.; Yang, J.; Wong, G. K. In *Nonlinear Optical Effects in Organic Polymers*; Messier, J., Kajar, F., Prasad, P., Ulrich, D., Eds.; Kluwer Academic Publishers: Dordrecht, 1989; pp 173–183. (d) Hubbard, M. A.; Minami, N.; Ye, C.; Marks, T. J.; Yang, J.; Wong, G. K. *SPIE Proc.* **1989**, *971*, 136–143.

(2) Singer, K. D.; Kuzyk, M. G.; Holland, W. R.; Sohn, J. E.; Lalama, S. J.; Commizzoli, R. B.; Katz, H. E.; Schilling, M. L. *Appl. Phys. Lett.* **1988**, *53*, 1800–1802.

(3) (a) Eich, M.; Sen, A.; Looser, H.; Yoon, D. Y.; Bjorklund, G. C.; Twieg, R.; Swalen, J. D. *SPIE Proc.* **1989**, *971*, 128–135. (b) Eich, M.; Sen, A.; Looser, H.; Bjorklund, G. C.; Swalen, J. D.; Twieg, R.; Yoon, D. Y. *J. Appl. Phys.* **1989**, *66*, 2559–2567.

(4) (a) Messier, J., Kajar, F., Prasad, P., Ulrich, D., Eds. *Nonlinear Optical Effects in Organic Polymers*; Kluwer Academic Publishers: Dordrecht, 1989. (b) Khanarian, G., Ed. Nonlinear Optical Properties of Organic Materials. *SPIE Proc.* **1989**, *971*. (c) Heeger, A. J., Orenstein, J., Ulrich, D. R., Eds. Nonlinear Optical Properties of Polymers. *Mater. Res. Soc. Symp. Proc.* **1988**, *109*. (d) Chemla, D. S., Zyss, J., Eds. *Nonlinear Optical Properties of Organic Molecules and Crystals*; Academic Press: New York, 1987; Vols. 1 and 2. (e) Zyss, J. *J. Mol. Electron.* **1985**, *1*, 25–56. (f) Williams, D. J. *Angew. Chem., Int. Ed. Engl.* **1984**, *23*, 690–703.

0897-4756/90/2802-0229$02.50/0

Scheme I

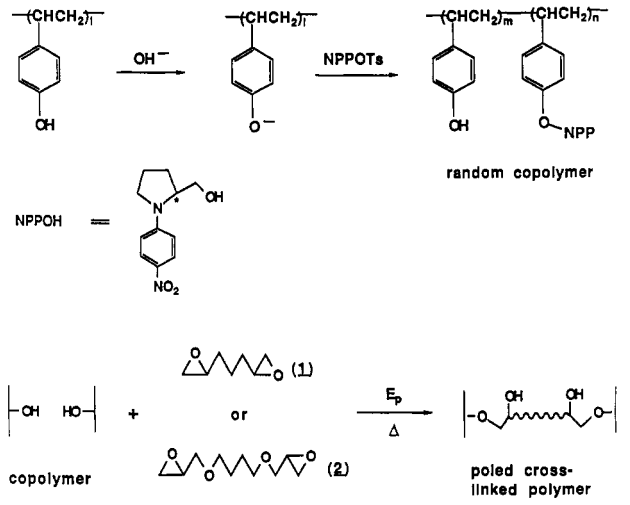

SHG temporal stability, have not been microscopically well-understood or subject to additional chemical control in such materials. The latter issue might, in principle, be addressable by using a chromophore-functionalized macromolecule having additional chemical functionality, and we report here[7] on the promising results of *simultaneously* poling and chemically cross-linking[8] a chromophore-functionalized NLO polymer.

Poly(*p*-hydroxystyrene) ($\bar{M}_W \approx 6000$, $T_g = 155$ °C) was functionalized[1b] with the well-characterized model chromophore *N*-(4-nitrophenyl)-(*S*)-prolinol[9] (NPP; 16% of phenol rings) as shown in Scheme I. The product was purified by repeated benzene precipitation from THF solutions and filtration through a short silica gel column. Purity was checked by elemental analysis, 400-MHz ^{1}H NMR and FT-IR spectroscopy.[10] In a class 100 laminar-flow clean hood, 1–2-μm (PS)O–NPP films were cast onto ITO-coated conductive glass from multiply filtered THF solutions also containing measured quantities of 1,2,7,8-diepoxyoctane (**1**) or 1,4-butanediol diglycidyl ether (**2**, Scheme I). Optimum thermal cross-linking conditions (vide infra) were established by independent experiments, monitored by FT-IR spectroscopy of films cast on KBr plates. Cross-linking is accompanied by diminution of the epoxy ring vibrational mode at 907–913 cm^{-1} and the concurrent appearance of an ether C–O stretching transition at 1040–1048 cm^{-1}.[11] The (PS)O–NPP/1,2 films were partially cured at 100 °C for 1 h under inert atmosphere and 100 °C/10^{-4} Torr for 24 h. As judged by FT-IR spectroscopy, this procedure effects partial cross-linking as well as removal of final traces of THF and other volatiles that deleteriously plasticize the matrix.[1b] The annealed films were next corona poled[2,12,13] (+3.0 to +4.0 kV; 1.0-cm needle-to-film distance) at 180 °C for 1 h. For optimum stoichiometries (vide infra), such thermal conditions induce high degrees of cross-linking (epoxide modes are undetectable in the IR),[14] while corona poling provides higher electric fields than contact poling techniques without facile dielectric breakdown.[12] The poled (PS)O–NPP/1,2 films were then cooled to room temperature and physically aged for 1 h prior to removal of the corona field. Such films are insoluble in all common organic solvents and far more resistant to cracking than non-cross-linked films. Good transparency characteristics are illustrated by the successful fabrication of (PS)O–NPP/1 waveguides.[15]

Table I. Second Harmonic Coefficients and Decay Parameters for Corona-Poled NPP-Functionalized Poly(*p*-hydroxystyrene) Films as a Function of Cross-Linking[a]

cross-linking agent	stoichiometry diepoxide/OH[b]	$10^9 d_{33}$,[c] esu	τ_1,[d] days	τ_2,[e] days
none		8.8	26	30
none		8.6[f]	36[f]	26[f]
1	0.50	7.0	79	100
2	0.25	3.8	18	74
2	0.50	5.5	20	53
2	0.75	2.1	11	51
2	1.00	1.4	9	46

[a] Films poled at 180 °C unless otherwise indicated. [b] Equivalents of diepoxide cross-linking agent per equivalent of available phenol OH. [c] At $\lambda = 1.064$ μm. [d] Short-term SHG decay constant from a least-squares fit to eq 1. Data taken at 25 °C. [e] Long-term SHG decay constant from a least-squares fit to eq 1. Data taken at 25 °C. [f] Poled at 150 °C.

Second harmonic coefficients (d_{33}) of the (PS)O–NPP/1 films were measured at 1.064 μm by using the instrumentation and calibration techniques reported elsewhere.[1] Analysis of the angular dependence of $I^{2\omega}$ utilized the standard formalism of Jerphagnon and Kurtz for uniaxial materials.[16] The additional assumption that $d_{31} = d_{24} = d_{15} = d_{33}/3$ has been verified for other poled, chromophore-functionalized polymers.[1c] No SHG was observed for unpoled specimens. The temporal characteristics of d_{33} were measured for film samples stored in a desiccator at room temperature. Data were fit by least-squares techniques to the phenomenological biexponential expression of eq 1.[1]

$$d_{33} = Ae^{-t/\tau_1} + Be^{-t/\tau_2} \quad (1)$$

In Table I are set out d_{33}, τ_1, and τ_2 data for (PS)O–NPP films as a function of cross-linking methodology. In viewing such data, it is expected that the statistical, molecular gas description of chromophore response[17] should hold over a fairly wide range of conditions[1] (eqs 2 and 3).

(5) (a) Struik, L. C. E. *Physical Aging in Amorphous Polymers and Other Materials*; Elsevier: Amsterdam, 1978. (b) Victor, J. G.; Torkelson, J. M. *Macromolecules* **1987**, *20*, 2241–2250. (c) Yu, W.-C., Sung, C. S. P.; Robertson, R. E. *Macromolecules* **1988**, *21*, 355–364, and references therein.

(6) (a) Hampsch, H. L.; Yang, J.; Wong, G. K.; Torkelson, J. M. *Macromolecules* **1988**, *21*, 526–528. (b) Hampsch, H. L.; Yang, J.; Wong, G. K.; Torkelson, J. M. *Polym. Commun.* **1989**, *30*, 40–43.

(7) Communicated in part at the "Symposium on Electroresponsive Molecular and Polymeric Systems", Brookhaven National Laboratory, Oct 25–27, 1989.

(8) For other recently reported cross-linking approaches not involving functionalized polymers, see ref 1d and the following: (a) Hubbard, M. A.; Marks, T. J.; Yang, J.; Wong, G. K. *Chem. Mater.* **1989**, *1*, 167–169. (b) Eich, M.; Reck, B.; Yoon, D. Y.; Wilson, C. G.; Bjorklund, G. C. *J. Appl. Phys.* **1989**, *66*, 3241–3247.

(9) (a) Zyss, J.; Nicoud, J. F.; Coquillay, M. *J. Chem. Phys.* **1984**, *81*, 4160–4167. (b) Barzoukas, M.; Josse, D.; Fremaux, P.; Zyss, J.; Nicoud, J. F.; Morley, J. *J. Opt. Soc. Am. B* **1987**, *4*, 977–986.

(10) Anal. Calcd for $(C_8H_8O)_{0.84}(C_{19}H_{20}N_2O_3)_{0.16}$: C, 76.70; H, 6.54; N, 2.93. Found: C, 76.30; H, 7.01; N, 2.50.

(11) (a) McAdams, L. V.; Gannon, J. A. In *Encyclopedia of Polymer Science and Engineering*; Wiley: New York, 1986; Vol. 6, pp 322–382, and references therein. (b) Mertzel, E.; Koenig, J. L. *Adv. Polym. Sci.* **1985**, *75*, 74–112.

(12) Comizzoli, R. B. *J. Electrochem. Soc.* **1987**, *134*, 424–429, and references therein.

(13) Dai, D.; Marks, T. J.; Yang, J.; Lundquist, P. M.; Wong, G. K., *Macromolecules*, in press.

(14) Temperatures greater than 220 °C lead to substantial thermal decomposition of the films.

(15) Park, J.; Marks, T. J.; Yang, J.; Lundquist, P. M.; Wong, G. K., unpublished results.

(16) Jerphagnon, J.; Kurtz, S. K. *J. Appl. Phys.* **1970**, *41*, 1667–1681.

(17) (a) Singer, K. D.; Sohn, J. E.; Lalama, S. J. *Appl. Phys. Lett.* **1986**, *49*, 248–250. (b) Singer, K. D.; Kuzyk, M. G.; Sohn, J. E. *J. Opt. Soc. Am. B* **1987**, *4*, 968–975.

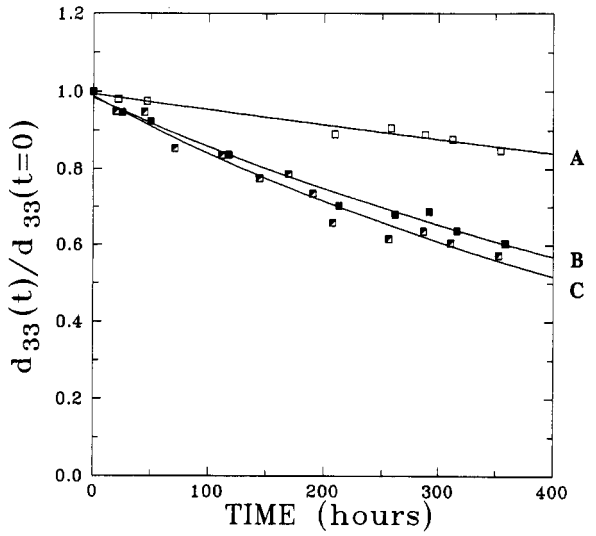

Figure 1. Temporal characteristics of the second harmonic coefficient d_{33} for corona-poled (PS)O–NPP films. (A) Simultaneously poled (180 °C) and cross-linked with 0.50 equiv of 1,2,7,8-diepoxyoctane/phenol OH. (B) Poled at 180 °C. (C) Poled at 150 °C. The solid lines are least-squares fits to eq 1, yielding the parameters in Table I.

$$d_{33} = \frac{1}{2}Nf^{2\omega}f^{\omega}f^{\omega}\beta_{zzz}L_3(p) \quad (2)$$

$$p = f^{\circ}\mu E_p/(kT) \quad (3)$$

Here N is the chromophore number density, the f's are local field factors, L_3 is the third-order Langevin function, μ is the chromophore dipole moment, and E_p is the poling field. Also note that τ_1, τ_2 values are typically depressed as poling fields increase,[1c] reasonably reflecting the greater restoring forces as the chromophore dipole system is driven further from thermodynamic equilibrium.

With the above caveats in mind, it can be seen in Table I that the present, corona-poled d_{33} values are generally higher than previously achieved for contact-poled (PS)O–NPP samples at comparable or higher functionalization levels and are also in excess of values reported for cross-linked guest–host systems.[1b,c,8a] This is to be expected if eqs 2 and 3 apply. Equally important, Table I shows that SHG efficiency is not adversely affected by the cross-linking process. In regard to d_{33} temporal stability, Figure 1 compares the effects of simultaneously corona poling and cross-linking (PS)O–NPP with 0.5 equiv of 1/available phenol OH group to two films poled in an essentially identical manner but not cross-linked. The increase in SHG temporal stability is clearly rather substantial and translates into 3.0-fold and 3.3-fold increases in τ_1 and τ_2, respectively.[18] The effect of the epoxy cross-linking/densification process[19] on chromophore mobility[8a,20] will be a complex function of cross-linking temperature, stoichiometry, and cross-linking agent. Figure 2 illustrates the effect on the $d_{33}(t)$ τ_2 parameter of varying the stoichiometry of cross-linking agent for constant poling procedure. It can be seen that τ_2 rises to a maximum at relatively low

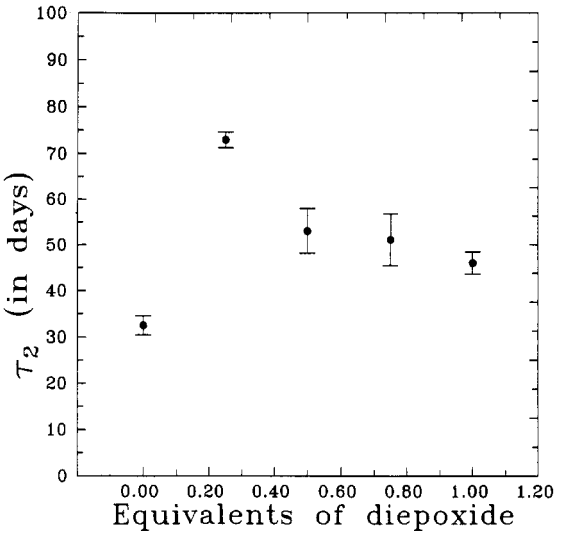

Figure 2. Long-term decay parameters (eq 1) for d_{33} of poled (PS)O–NPP films simultaneously corona poled and cross-linked with the indicated equivalents of 1,4-butanediol diglycidyl ether/equivalents of available phenol OH.

diepoxide/available phenol OH ratios and then gradually falls at higher diepoxide ratios. FT-IR indicates unreacted epoxide functionalities (incomplete cross-linking) at the higher 2/OH ratios, and it is reasonable that dangling, half-reacted epoxide side chains will have a plasticizing effect on the chromophore/polymer matrix. At 2/OH ratios greater than ca. 0.5, the matrix becomes opaque after casting and curing, indicating phase separation. This leads to a decrease in the apparent d_{33}. Differences in τ_1, τ_2 parameters for matrices cross-linked by 1 and 2 (Table I) can be attributed to differences in chain flexibility of these reagents.

In summary, these results demonstrate that the temporal stability of poling-induced chromophore alignment in chromophore-functionalized NLO polymers can be significantly enhanced by chemical cross-linking, effected concurrently with corona poling.

Acknowledgment. This research was supported by the NSF-MRL program through the Materials Research Center of Northwestern University (Grant DMR8821571) and by the Air Force Office of Scientific Research (Contract AFOSR-88-C-0122).

Registry No. 1, 2426-07-5; 2, 2425-79-8.

(18) It is noted that the present τ_1 values are somewhat larger than observed in earlier studies of contact poled (PS)O–NPP films.[1b,c] In agreement with those findings, we attribute this to the further loss of plasticizing impurities at the present higher annealing temperatures.

(19) (a) Kloosterboer, J. G. *Adv. Polym. Sci.* **1988**, *84*, 3–61. (b) Oleinik, E. F. *Adv. Polym. Sci.* **1986**, *80*, 49–99. (c) Dusek, K. *Adv. Polym. Sci.* **1986**, *78*, 1–59. (d) Rozenberg, B. A. *Adv. Polym. Sci.* **1986**, *75*, 73–114. (e) Morgan, R. J. *Adv. Polym. Sci.* **1985**, *72*, 1–43.

(20) (a) Yu, W.-E.; Sung, C. S. P. *Macromolecules* **1988**, *21*, 365–371, and references therein. (b) Sung, C. S. P.; Pyun, E.; Sun, H.-L. *Macromolecules* **1986**, *19*, 3922–3929.